UDC 621. 224. 01:532. 528

DEVELOPMENT OF MODEL TURBINE BY COMPUTERIZED NUMERICAL EXPERIMENTS

Takashi Kubota
Seiji Takimoto
Hiroyuki Aoki

I. INTRODUCTION

Since the hydro-electric power plants are used to cover quick load variation, the hydraulic turbines and pump-turbines work during most of the time under a condition away from the best efficiency point. The operating conditions at the maximum/minimum heads are also largely deviated from the best efficiency point in the power plants where the head variation is noticeable. Under these operating conditions, the internal flow through the runner, wicket gates, and stay vanes is no longer uniform, but it shows a complicated flow pattern. As a result, not only the performance deteriorates but also such cavitation, vibration, and noise that have not been predicted from the past experience, come into question.

On the other hand, a great deal of effort continues to minimize the hydraulic losses to an extreme limit for the purpose of improving the performance of the hydro-turbine and pump-turbine. For this purpose, the efficiency characteristics, turbine discharge, pumping head, etc. must be predicted as accurately and rapidly as possible in the course of the design and planning stages.

In order to examine these hydraulic problems and execute the performance prediction, the trial and error model testings have continuously been adopted as a major approach. Since the selection of hydrofoils for runner, wicket gates, stay vanes, etc. requires a long experience and accumulated knowledge, repetitions of many model tests for combinations of various design parameters require a long development period and considerable costs plus man-power. Such a classical procedure alone is, therefore, inevitably limited to develop the hydro-turbine and pump-turbine efficiently.

Computer programs analyzing the flow through the hydro-turbine have developed as an up-to-dated approach. Now, the performance prediction based on the flow analysis computer programs has been put into practical use as a result of comparing computerized numerical experiment results with model test results measured in the hydraulic laboratory. This paper outlines the flow analysis computer programs for hydro-turbine and demonstrates the effectiveness of performance prediction by computerized numerical experiment.

II. FLOW ANALYSIS COMPUTER PROGRAMS

As high-speed, large-scaled engineering computers shows a rapid progress, the numerical computing analysis techniques have advanced to permit simulating the internal flow through the hydro-turbine numerically. The outline and some features of the computer programs for analyzing the flow through the runner, stay vanes, and wicket gates will be described as follows:

1. Runner flow analysis computer program (RUNFLAS)

This computer program analyze the quasi-three-dimensional flow through the runner as combinations of two two-dimensional flows on the crown-to-band plane (*Fig. 1*) and on the blade-to-blade surfaces (*Fig. 2*).

The crown-to-band flow analysis is based on the stream filament method while the blade-to-blade flow analysis employs the singularity method in which vortex rows equivalent to the blade circulation are arranged on the camber line of the hydrofoil[3].

Unlike such an approach as to solve the stream function by means of the finite difference and/or finite element method, this approach features as follows;

(1) Since the flow angle discharged from the turbine runner can be computed, turbine discharge and magnitude of whirl flow at the runner outlet can be obtained.

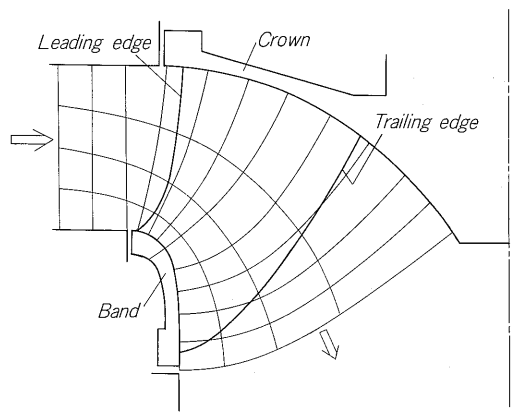

Fig. 1 Crown-to-band plane

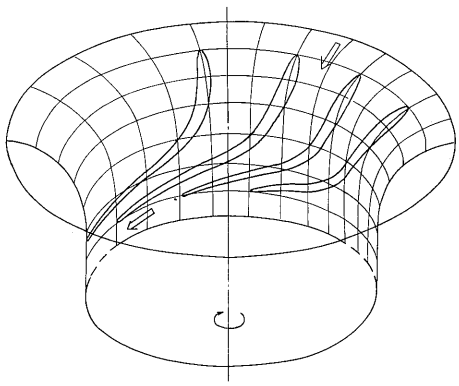

Fig. 2 Blade-to-blade surface

(2) The impeller head of pump can be computed, and this serves as an input condition to STAFLAS to analyze the flow through stay vanes and wicket gates described later.

2. Stay vanes/wicket gates flow analysis computer program (STAFLAS)

This program is an extended RUNFLAS method to analyze the flow of the double circular cascades comprising stay vanes and wicket gates. Its major features are as shown below.

(1) Since the flow discharge angle from wicket gates can be computed, the velocity triangle at runner inlet can be examined. Thus, input data to RUNFLAS (inflow condition to runner) can be obtained.

(2) The allocation of flow rate from front cascade to rear cascade can be calculated. In the turbine flow shown in *Fig. 3*, for example, the ratio of discharge from the channel outlet (A~C) between stay vanes to that into the channel (A~B) between stay vane and wicket gate can be obtained, and this can be utilized as an input value to the computer program by means of the stream function method described later.

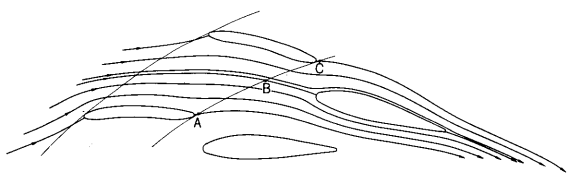

Fig. 3 Flow allocation between stay vanes and wicket gates

3. Blade-to-blade flow computer programs for thick hydrofoils (BLADAS, GATAS, LEADED)

Since RUNFLAS and STAFLAS described above are based on the thin blade theory, a considerable computational error results when computing the flow around the leading edge of blade where the gradient of thickness distribution along camber line is large, and the flow around the thick blade like wicket gate leaf. Contrary, the computer programs solving the stream function between blade-to-blade by means of the finite difference method[4] can compute the flow velocity/static pressure distribution around thick blades accurately, though the discharge angle as well as the inflow angle must be inputted as boundary conditions. The BLADAS is applicable to the flow analysis of a single cascade like runner, while GATAS is available for the double cascades comprising stay vanes and wicket gates. In addition, LEADED has been developed to analyze the leading and/or trailing edges of blades in detail by magnifying the concerning region.

III. COMPUTERIZED PREDICTION OF TURBINE CHARACTERISTICS

1. Runner inlet cavitation and incidence angle

In *Fig. 4* indicate the typical hydraulic characteristics of the model Francis turbine. The rotating speed-ratio $n_{11}/n_{11\,BEP}$ (the ratio of unit speed to the value at the best efficiency point) is plotted on the abscissa, while the discharge-ratio $Q_{11}/Q_{11\,BEP}$ on the ordinate. On the left side of line ① in the figure, the flow incidence angle relative to the runner vane inlet increases, causing cavitation, flow separation and noise to be produced on the low pressure surface of vane inlet. On the right side of line ②, the negative incidence angle increases, causing noise to be produced by separating flow from the inlet high pressure surface. In other words, as for the inflow condition to the runner inlet, the region bounded by lines ① and ② ensures the smooth operation.

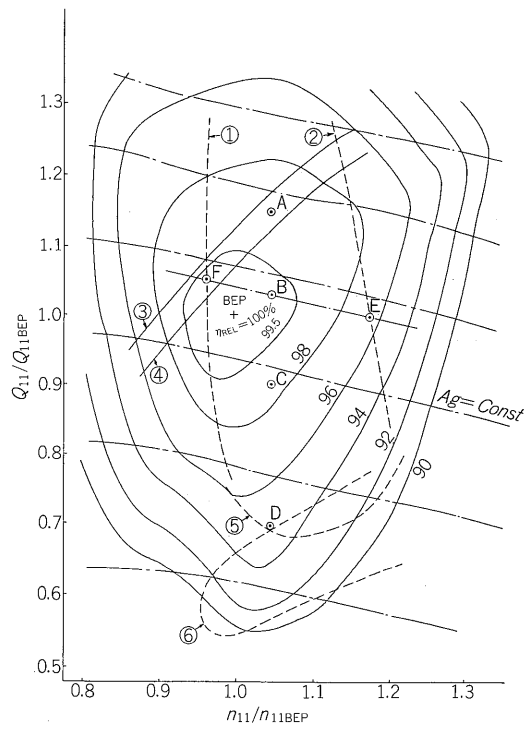

Fig 4. Turbine characteristics

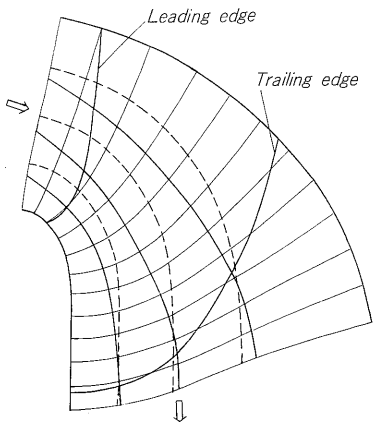

(a) Operating point : F

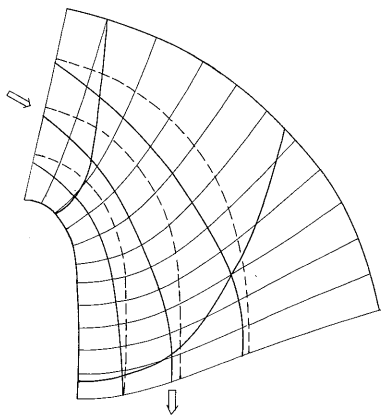

(b) Operating point : E

Fig. 5 Crown-to-band streamlines

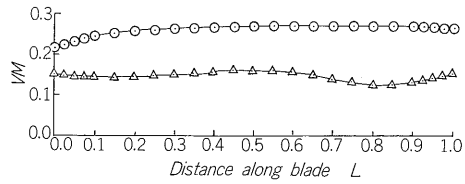

(a) Crowm

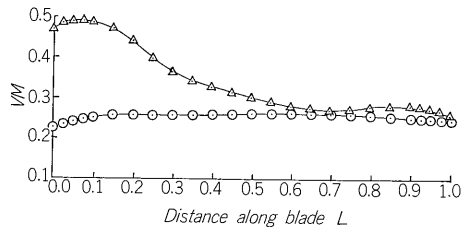

(b) Band

Fig. 6 Meridional velocity distribution

It is, therefore, preferable for designing a turbine to place a frequent operating range within the region between ① and ② Since the cavitation on the left side of line ① tends to develop rapidly on 'low' pressure surface, in particular, it is apt to cause cavitation damage. Accordingly, the use on the region far left side as viewed from line ① must be avoided as much as possible. On the other hand, since the cavitation on the right side of line ② is produced on 'high' pressure surface, it does not necessarily cause a damage.

Figs. 5~8 indicate computerized numerical experiment results when changing unit speed (operating points E and F in *Fig. 4*) with the gate opening fixed constant. The dotted lines in *Fig. 5* divide the meridional crown-to-band channel into four partial runners, each having an equal cross area. Since these dotted lines (so called classical streamlines) can be determined geometrically, they are identical to each other at operating points E and F, irrespective of the operating conditions.

On the other hand, the solid lines in *Fig. 5* indicate the meridional steamlines computed by RUNFLAS. These computerized solid lines are, as a whole, deviated toward the band as compared with the classical dotted lines, and this tendency is noticeable in such a range that curvature of band is large. This is because that corvature of band is larger than that of crown, and flow is accelerated on the inner (band) wall of meridional channle. Also, the solid lines at operating point E are deviated toward the band more than those at point F, because that unit speed of E is larger than that of F, and resultantly, the centrifugal force around the rotating axis is larger at operating point E as compared with point F.

As a result, the computerized meridional flow velocity along the inner wall of crown and band becomes as shown by mark △ in *Fig. 6*. Mark ⊙ indicates the classical meridional velocity when dividing the crown-to-band channel into equi-areal partial runners. The computerized velocity marked with △ decelerates on the crown and accelerates on the band as compared with the classical velocity marked with ⊙.

From the above phenomena, the flow velocity triangles at the crown/band inlet can be shown by *Fig. 7*. Relative inflow angle δ_1 does not change much at the band inlet even if unit speed (or, peripheral velocity) increases, but δ_1 tends to change largely at the crown inlet becuase of small meridional velocity.

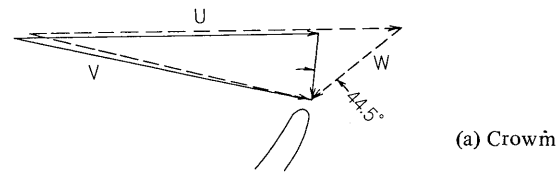

(a) Crowm

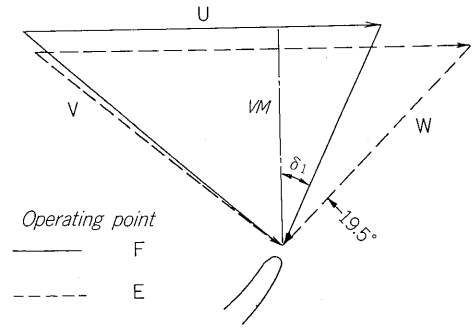

(b) Band

Fig. 7 Velocity triangle

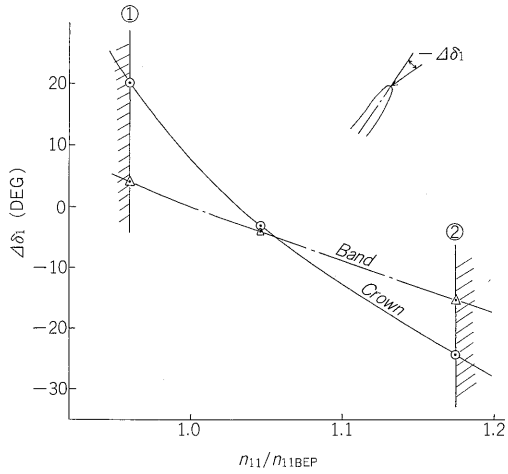

Fig. 8 Flow incidence angles

As shown in *Fig. 8*, the incidence angle changes more rapidly on the crown than on the band with the speed variation. It reveals that, in the case, flow separates from the crown on both lines ① and ② Thus, the cavitation free region at runner inlet can be predicted by RUNFLAS when computerized results of incidence angle are, in advance, correlated with lines ① and ② of past model test results.

2. Runner outlet cavitation and blade pressure distribution

If the test cavitation factor (test sigma) of a model turbine is reduced while keeping the test head constant under the full load operating condition, it may be observed visually that the cavitation bubbles occur on the low pressure surface at runner vane outlet from the band side usually when the test sigma reaches a certain value. The cavitation beginning sigma σ_{BEG} obtained can be plotted as the solid line in *Fig. 9* with reference to the discharge. If the prototype turbine is operated for a long time under the severe cavitating state, harmful cavitation damage may result. It is, therefore, necessary to predict the beginning sigma in the course of design stage in order to examine the installation height of hydro-turbine.

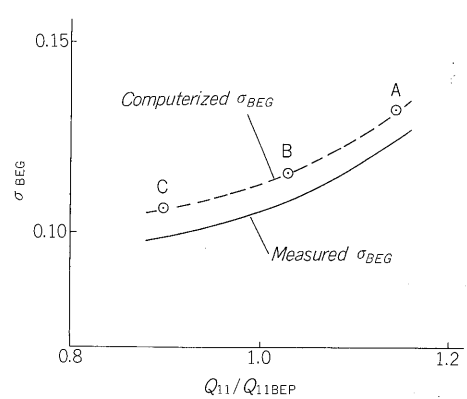

Fig. 9 Cavitation beginning sigma

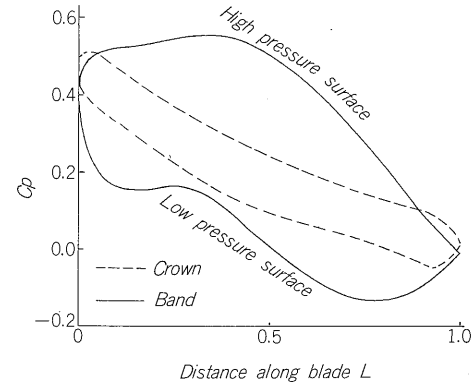

Fig. 10 Pressure distribution around turbine blade

Since the cavitation occurs at a location where the static pressure on the blade surface reaches minimum, the pressure distribution on the surface of runner vane must be analyzed for this study. *Fig. 10* indicates an example of computerized pressure distribution around blade surface at operating point A in *Fig. 4*. The abscissa indicates the distance measured from the inlet along the blade profile. Pressure coefficient *Cp* on the ordinate indicates the static pressure on the blade surface referenced from the total pressure at runner outlet, and it can be defined by the following expression.

$$Cp \equiv \frac{P/\gamma - P_{T2}/\gamma}{H} \fallingdotseq \frac{P/\gamma - (H_a - H_s)}{H}$$

where,
- P/γ: Blade static pressure head (mAq, abs)
- P_{T2}/γ: Total pressure head at runner outlet (mAq, abs) $\fallingdotseq H_a - H_s$
- H: Net head (m)
- H_a: Atmospheric pressure head (mAq, abs)
- H_s: Suction head (m)

Assuming that cavitation occurs at the location when the blade minimum pressure reaches down to the vapor pressure of water H_v (mAq, abs), cavitation beginning

$$Cp\ \min = \frac{H_v - (P_{T2}/\gamma)_{BEG}}{H} \fallingdotseq \frac{H_v - (H_a - H_s)_{BEG}}{H}$$

$$= -\sigma_{BEG}$$

sigma can, therefore, be obtained by reversing the sign of blade minimum pressure coefficient Cp_{min} picked up from *Fig. 10*.

The computerized cavitation beginning sigmas obtained from Cp_{min} at points A~C in *Fig. 4* are shown by mark ⊙ in *Fig. 9*. Thus, an occurrence of cavitation can be predicted by previously correlating computerized numerical experiment results with past model test results.

3. Pressure surge in draft tube and runner outlet whirl

On the upper side of line ③ in *Fig. 4*, whirl flow is

produced at runner outlet in the direction opposite to the runner rotation, and a vortex core can be observed visually at the center of upper draft tube. On the lower side of line ④, on the other hand, a vortex core appears due to the whirl flow in the same direction as that of the runner rotation. Accordingly, smooth whirl-free flow can be seen in the vicinity of runner crown outlet within the region bounded by lines ③ and ④. In a region bounded by line ⑥, the vortex core is developed to be a dead-water core, which fluctuates eccentrically in the upper draft tube to produce hydraulic pressure pulsation and vibration[5].

The ratio of whirl to axial flow momentum at the runner outlet serves as a parameter controlling such a pressure surge in the draft tube[6]. This can be calculated from RUNFLAS results as shown by the following equation.

$$MR_2 = \frac{\Sigma \Delta Qi \cdot Ri \cdot Vui}{\Sigma \Delta Qi \cdot Ri \cdot Vmi}$$

where, suffix i: Identification number of partial runner
ΔQ: Discharge through partial runner
R: Radius at partial runner outlet
V_u: Whirl velocity at partial runner outlet

Fig. 11 indicates the calculation results of this MR_2 at operating points A~D in *Fig. 4* comparing with the amplitude of pressure pulsation (peak-to-peak) measured at the upper draft tube of model turbine. Thus, the surging characteristics can be predicted by correlating computerized results of momentum ratio MR_2 with past model surge test results.

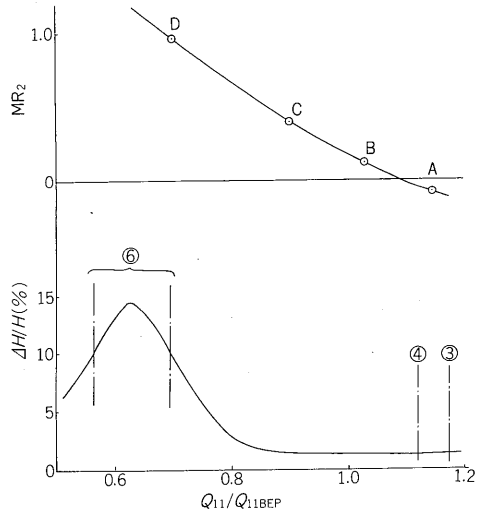

Fig. 11 Whirl to axial momentum ratio and pressure pulsation

4. Hydraulic loss analysis and performance prediction

The respective component hydraulic losses in the runner, wicket gates and stay vanes such as frictional loss on the blade surface, shock loss against blade inlet, wake loss at vane outlet, as well as the hydraulic losses in spiral casing and draft tube can be calculated by utilizing the above mentioned velocity/pressure/flow angle distributions[7]. Consequently, the integrated total hydraulic loss of the whole turbine can be obtained by adding the disc friction and leakage losses.

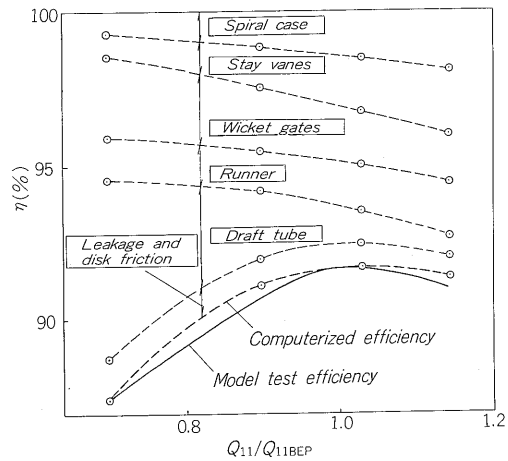

Fig. 12 Integration of component losses

Fig. 12 indicates calculation results of the component hydraulic losses at operating points A~D in *Fig. 4*. The total hydraulic loss curve integrated the component losses coincides fairly well with the model turbine efficiency curve in their tendencies, thus permitting the performance prediction.

IV. COMPUTERIZED PREDICTION OF PUMP CHARACTERISTICS

1. Impeller inlet cavitation

Fig. 13 indicates typical pump characteristics of low specific speed model pump-turbines. In the smaller discharge region on the left side of line ①, the flow incidence angle to the impeller inlet increases, and the static pressure on the low pressure surface at vane inlet decreases, causing the cavitation to occur. In the larger discharge region on the right side of line ②, on the other hand, the negative incidence angle increases, causing the cavitation to be produced from the high pressure surface at vane inlet. Accordingly, a smooth, cavitation-free operating condition can be obtained by selecting the installation height in such a manner that the installation sigma of prototype turbine is positioned on the upper region of lines ① and ②.

The cavitation beginning sigma of pump is exclusively determined by the discharge only. Computerized tests were, therefore, performed by changing the discharge at points A, B and C in *Fig. 13*.

Fig. 14 indicates the blade static pressure distribution computed by RUNFLAS/BLADAS. The cavitation beginning sigma is expressed by reversing the sign of the minimum value of static pressure coefficient Cp as described in clause (III. 2). The computerized beginning sigmas are shown by mark ⊙ in *Fig. 13*. These computerized results

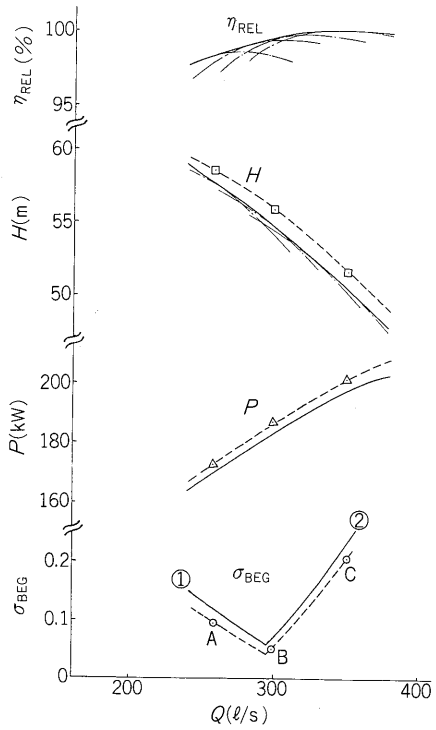

Fig. 13 Pump characteristics

show a good tendency similar to that of visual observation, and the beginning sigma can be predicted by numerical experiments.

2. Pump input power

It is necessary estimate the pumping input as compared with the generating output in the course of pump-turbine projection stage. The pumping input can be obtained by discharge Q (m^3/s), leakage flow ΔQ_L (m^3/s), impeller head, H_I (m), and disc frictional loss power ΔP_{FRIC} (kW) as follows;

$$P\,(\mathrm{kW}) = (\gamma/102) \cdot H_I \cdot (Q + \Delta Q_L) + \Delta P_{FRIC}$$

where, H_I can be obtained from the output data of RUNFLAS by the following equation.

$$H_I = (U_1 \cdot V_{u1} - U_2 \cdot V_{u2})/g$$

The pumping inputs thus calculated are shown by mark ⚠ in *Fig. 13*. The computerized inputs coincide with experi mental values in their tendencies quantitatively.

3. Pump head

Mark ⊡ in *Fig. 13* indicates the computerized total dynamic head obtained by subtracting the component hydraulic losses at the impeller, wicket gates, stay vanes, etc. from the impeller head by RUNFLAS described in the previous paragraph. The computerized head shows a tendency similar to that of the model test results, and it also shows that the head-discharge curve can be predicted by the numerical experiments.

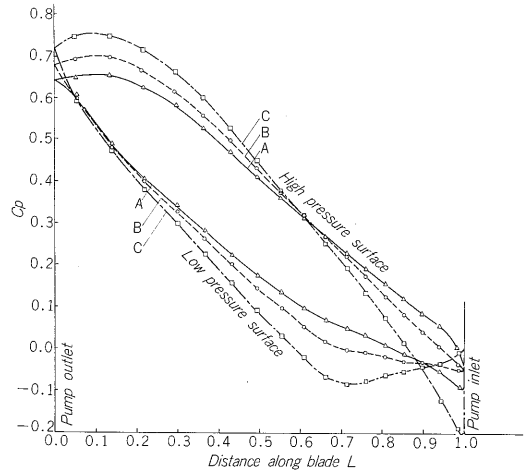

Fig. 14 Pressure distribution around impeller vane

V. CONCLUSION

As described above, an optimum design shape can be selected out of combinations of various design parameters by repeating numerical experiments using flow analysis computer programs. It is, however, difficult to predict accurately the performance at an operating point largely deviated from the design point by computerized numerical experiments, because of their restrictions in theory. On the other hand, the model testing procedure takes a much time to perform, but this procedure can accurately obtain the performance and vibration characteristics of the entire hydro-turbine and pump-turbine including the four quadrant characteristics.

Thus, the numerical experiments by no means supersedes the model tests, but these numerical experiments and model tests are supplementary to each other based on respective feautures. In this sense, the computerized flow analysis and model tests are said quite inseparable, and therefore, it may be considered that optimum turbine and pump-turbine can be developed by using them jointly and skillfully.

References

(1) J.T. Hamrick, A. Ginsburg and W.M. Osborn: Method of Analysis for Compressible Flow Through Mixed-Flow Centrifugal Impellers of Arbitrary Design, NACA Report 1082(1952)

(2) T. Katsanis : Use of Arbitrary Quasi-Orthogonals for Calculating Flow Distribution in the Meridional Plane of a Turbomachine, NASA TN D-2546 (1964)

(3) Y. Senoo and Y. Nakase: A Blade Theory of an Impeller with an Arbitrary Surface of Revolution, Journal of Eng. for power, Trans. ASME, Series A, Oct. (1971)

(4) For example, T. Katsanis: Computer Program for Calculating Velocities and Streamlines on a Blade-to-Blade Stream Surface of a Turbomachine, NASA TN D-4525 (1968)

(5) T. Kubota and H. Matsui: Cavitation Characteristics of Forced Vortex Core in the Flow of the Francis Turbine, Fuji Electric Review 18 (1972), No. 3

(6) U.J. Palde: Influence of Draft Tube Shape on Surging Characteristics of Reaction Turbines, B O R Report REC-ERC-72-24 (1972)

(7) T. Ida: Scale Effect Formulae and Corresponding Points on Water Turbine Characteristics, Report of Department of Technology, Kanagawa Univ., No. 14 (1976)